Beamforming Imaging in Cylindrical Structures Using Helicoidal Reflected SH Waves

ESTEBAN GUERRA-BRAVO and ARTURO BALTAZAR

ABSTRACT

Implementing guided wave imaging (GWI) for structural health monitoring (SHM) of cylindrical structures can be enhanced by simplifying the physics and utilizing all the information generated by wave interactions with the mechanical guide and discontinuities. A beamforming method for SH0 waves reflected from a trough-hole in a cylinder has been developed. This method considers the mode conversion from T(0,1) to SH0 waves, which follow direct and helical paths before converting back to torsional waves. The use of helical paths enables the deployment of an array of sensors distributed along a section of the cylinder's circumference. Indeed, signal identification and integration into a beamforming scheme present challenges due to the multiple trajectories that propagate around the cylinder. The objectives of the numerical analysis are threefold: first, to model the propagation and interaction of torsional waves with a discontinuity; second, to numerically identify the helicoidal wave trajectories for full rotations (orders); and third, to develop and implement a frequency-domain MUSIC beamforming algorithm adapted for cylindrical structures. The results demonstrate the ability to reconstruct the defect's position and orientation. These findings highlight the potential of the proposed method for accurate defect localization in cylindrical structures.

INTRODUCTION

Guided waves provide a promising method for inspecting long sections of cylindrical structures, such as pipes, by propagating along the structure and reflecting off discontinuities, which aids in defect detection [1, 2]. Among the different guided wave modes available, shear horizontal (SH0) waves are particularly advantageous because they exhibit low dispersion and reduced attenuation, even in environments where the structure is in contact with liquids, making them highly suitable for engineering applications [3, 4].

Esteban Guerra-Bravo, email: esteban.guerrabravo@gmail.com
Universidad Politecnica de Ramos Arizpe (UPRA), Ramos Arizpe, Coahuila, Mexico.
Arturo Baltazar, email: arturo.baltazar@cinvestav.edu.mx
Robotics and Advanced Manufacturing Program, CINVESTAV-Saltillo, Ramos Arizpe, Coahuila, Mexico

In cylindrical structures, the equivalent SH0 mode is the torsional T(0,1), which has in-plane angular displacements. Upon encountering a discontinuity, T(0,1) waves scatter part of their energy in all directions around the cylinder, resulting in a complex circumferential wavefront distribution. This behavior contrasts with the scattering observed in planar structures, where wavefronts typically propagate along straight paths. In cylindrical structures, the scattered wavefronts follow the curvature of the surface. This scattering leads to wavefronts surrounding the cylinder, which can be viewed as scattered wavefronts traveling along multiple paths before reaching a transducer, and these paths, depending on the number of revolutions, can be interpreted as helical trajectories. The generation of SH0 waves through the interaction of the T(0,1) mode with discontinuities, such as through-holes and cracks, has also been studied [5–7].

An approach for damage imaging in pipes is the tomography-based technique, which uses transducer arrays arranged in full-ring configurations around the inspection region [8–10]. These methods typically require at least two ring arrays positioned at different axial locations along the pipe to enable transmission and reception. Beamforming, initially designed for volumetric waves, offers a simpler alternative for defect localization, as it does not require sequential actuation or multiple arrays like tomography-based techniques. Instead, it processes recorded signals from a sensor array to estimate the location of reflected wavefronts. To enhance the accuracy of wave source localization, spectral methods such as the Multiple Signal Classification (MUSIC) algorithm have been explored [11].

The main objective of this study is to develop a beamforming algorithm to localize trough-hole discontinuities in cylindrical structures using the scattered SH-waves. The interaction of an excited T(0,1) torsional mode with a discontinuity in a hollow cylinder was studied using FEM simulations. The resulting wavefields were analyzed to track the helicoidal paths of reflected SH modes. The recorded wavefronts were processed in the frequency domain using a beamforming technique formulated in cylindrical coordinates. Imaging was performed through a modified MUSIC algorithm. The proposed approach aims to enable defect localization without requiring a complete circumferential sensor ring.

GUIDED WAVES IN CYLINDRICAL STRUCTURES

Torsional guided waves, particularly the fundamental mode T(0,1), propagate along cylindrical structures with minimal dispersion and in-plane angular displacements. This mode is directly related to the SH0 wave in plates, as both exhibit non-dispersive behavior and share the same phase velocity, as shown by the overlapping dispersion curves in Figure 1. These characteristics make them useful for structural health monitoring (SHM) in pipes and other cylindrical components. However, when encountering a discontinuity, such as a crack or a notch, the incident wave undergoes scattering, redistributing energy in various directions around the cylinder. When a T(0,1) wave interacts with a defect, part of the energy is reflected as SH0 waves scattered circumferentially [5]. Unlike in planar structures, where scattered wavefronts propagate in straight surface paths, in cylindrical geometries, the scattered waves expand around the circumference. As a result, wave energy can travel along multiple paths before reaching a sensor array. These helical trajectories result in wavefronts arriving at the sensor array at different times,

depending on the number of circumferential cycles completed.

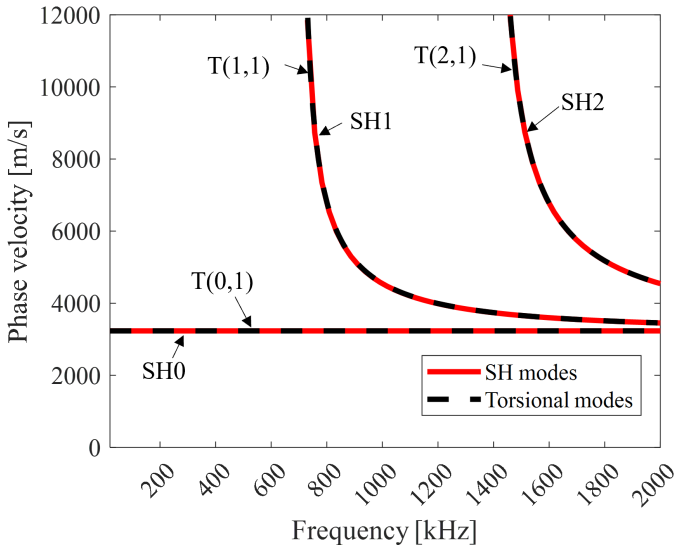

Figure 1. Comparison between SH dispersion curves in a plate and torsional dispersion curves in a hollow cylinder.

Figure 2 shows numerical FEM results illustrating the propagation of an SH0 wave in a hollow cylinder at different time steps. This behavior results in the formation of multiple wavefronts arriving at the sensor array from different directions, despite originating from a single source, making the implementation of imaging algorithms based on beamforming more challenging.

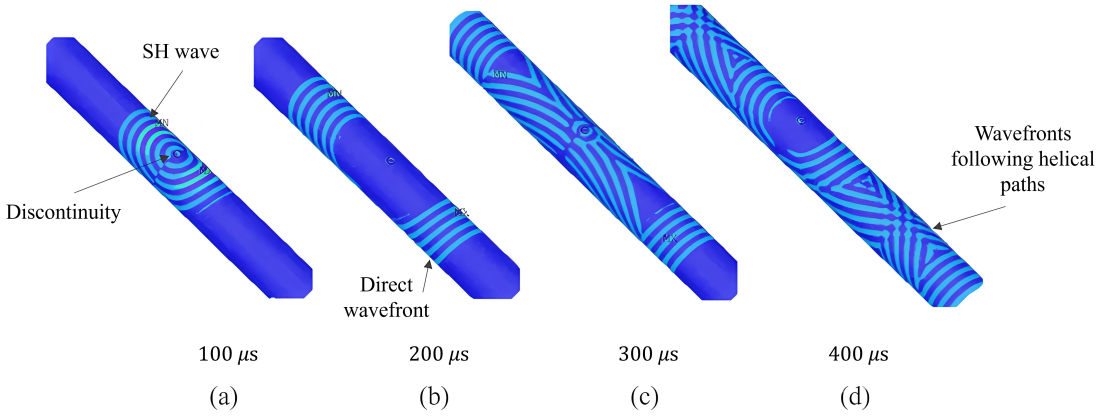

Figure 2. Numerical results of SH0 wave generated by a circular discontinuity in a hollow cylinder at different time steps (a) $100\mu s$, (b) $200\mu s$, (c) $300\mu s$, (d) $400\mu s$.

To better analyze the wave paths, the cylindrical domain can be conceptually unwrapped. In this representation, the direct path is a straight trajectory, whereas the helical path appears as diagonal propagation, showing how wavefronts can reach the transducers after completing one or more revolutions around the cylinder. However, since the wavefronts arrive from different directions, it is necessary to separate them before beamforming is implemented.

METHODOLOGY

Finite Element Model

A numerical model was developed in ANSYS APDL to generate synthetic signals for testing and validating an image reconstruction algorithm based on guided waves. The model consists of a cylindrical structure with a circular discontinuity placed at variable distances from a sensor array. A torsional mode T(0,1) is excited at one end of the cylinder. As this mode propagates along the structure and interacts with the discontinuity, part of its energy is converted into an SH0 wave that wraps helically around the cylinder. The resulting signals are captured by a sensor array located at $z = 0$, covering half of the cylinder's circumference. A schematic of the simulation setup is shown in Figure 3, and the simulation steps are outlined in pseudocode shown in Algorithm 1.

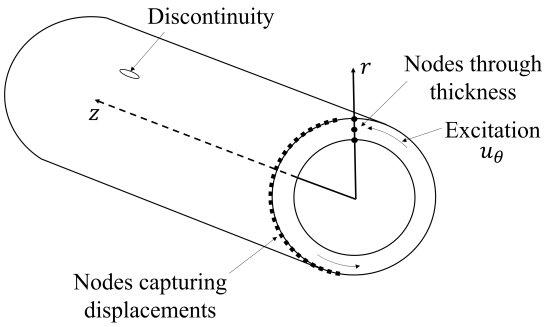

Figure 3. Scheme of the model showing the excitation, discontinuity, and sensor array.

The cylindrical structure was simulated as a pipe made of aluminum with a mean radius of $R = 0.1273$ m and a total length of $L = 1.5$ m. The excitation frequency was set to 60 kHz, and the mesh was defined with an element size equal to one-eighth of the wavelength ($\lambda/8$). Two elements were used through the thickness to ensure sufficient resolution. The mesh consisted of 20-node solid elements SOLID186. The total simulation time was 800 μs, with a time increment of 1 μs. The computational time for this simulation was approximately 4 hours, on a PC with Intel® Core™ i7-6820HQ CPU at 2.70 GHz.

Beamforming algorithm for SH0 with helical trajectories

To localize the source of wave reflections, a reconstruction image of the cylindrical surface is generated using the MUSIC algorithm adapted to cylindrical coordinates. The array consists of 8 sensors uniformly distributed along a quarter of the cylinder's circumference, with each sensor spaced by 10 degrees. The array is positioned on the outer surface of the cylinder. Since the cylinder has no boundaries except at its ends, the waves propagate around the cylinder, forming a continuous medium. This means that at a certain distance from the source, the wavefronts arriving at the array come from different directions. As a result, the algorithm treats these wavefronts as coming from multiple sources located at different angles. Peaks in the resulting image indicate the position of the discontinuity. The Algorithm 2 summarizes the steps of this process.

Algorithm 1 FEA procedure for wave propagation in a cylinder

1. Preprocessing: Simulation parameters and mesh generation
2. Input: geometry G, material M, mesh size h, excitation signal $f(t)$
$mesh \rightarrow$ mesh(G, h) with `Solid186` elements
K, $M \rightarrow$ assemble_matrices($mesh$, M)
Apply BC: $u_\theta = u_r = u_z = 0$ at $z = L$ *(boundary condition at the cylinder's end)*
3. Solution: Time-stepping procedure
for $t = 0$ to T step Δt **do**
3.1 Excitation: $F(t) \rightarrow$ apply_excitation($f(t)$) at $u(\theta, R, 0)$ for $\theta \in [0, 2\pi]$ *(tangential displacement at $z = 0$)*
3.2 Solve: $u(t + \Delta t) \rightarrow$ solve(K, M, $F(t)$, $u(t)$) *nodal displacements at time $t + \Delta t$*
3.3 Store: $store(u(t + \Delta t))$ *(save displacement results)*
end for
4. Postprocessing: postprocess(u) field of displacements at every time step

To aid the analysis, the cylindrical structure can be conceptually unwrapped into a planar representation. Figure 4 illustrates the propagation of a SH wave generated by a point source, showing the direct and helical paths.

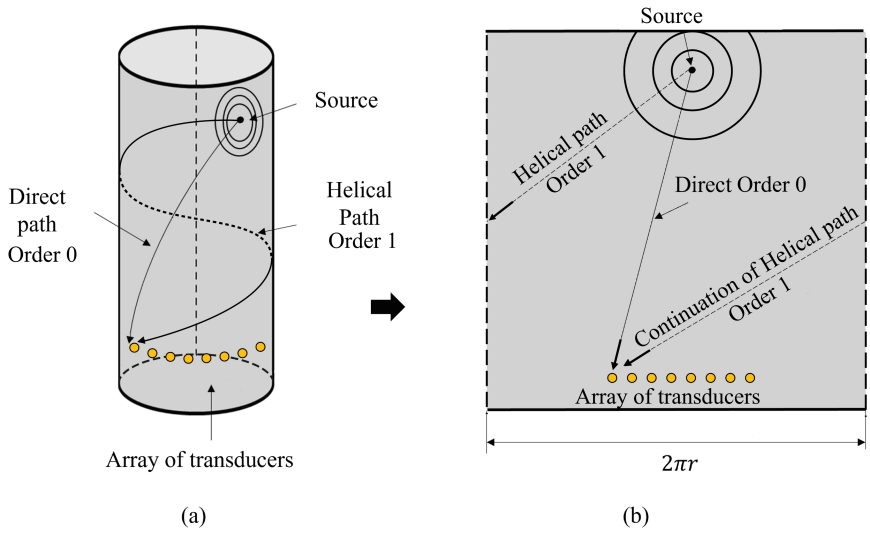

Figure 4. Propagation of SH waves from a point source. (a) Cylindrical view showing direct and helical wave paths. (b) Unwrapped view where wave paths appear as straight paths.

NUMERICAL RESULTS

Figure 5 shows an example of the signals captured by the array when the discontinuity is located at three different axial distances: 0.4 m, 0.6 m, and 0.8 m from the array. The first arriving wavefront, clearly visible in the three subplots, exhibits a curved

Algorithm 2 Image Reconstruction using MUSIC on a Cylindrical Surface

Input: sensor data $\mathbf{Y}$, frequency f, wave speed c, sensor positions $\mathbf{X}_m$
Apply FFT to $\mathbf{Y}$ to convert to the frequency domain
Estimate covariance matrix: $\mathbf{R} = \frac{1}{K}\sum_k \mathbf{Y}_k \mathbf{Y}_k^H$
Perform SVD: $\mathbf{R} = \mathbf{U}\mathbf{S}\mathbf{U}^H$
Extract noise subspace: $\mathbf{N} = [\mathbf{U}_{P+1}, \ldots, \mathbf{U}_N]$
for each reconstruction point (z, θ) ▷ θ is arc length: $\theta = R \cdot \phi$ **do**
    Compute delays τ_m and steering vector $\mathbf{s}$
    Compute MUSIC spectrum: $P_{\text{MUSIC}}(z, \theta) = \frac{1}{\|\mathbf{s}^H \mathbf{N}\mathbf{N}^H \mathbf{s}\|^2}$
end for
Output: MUSIC spectrum $P_{\text{MUSIC}}(z, \theta)$

shape (red box), consistent with a cylindrical wavefront (near field) originating from a localized scattering event. This enables the reconstruction of the source location based on differences in arrival time across the array. Following the first wavefront arrival (direct), additional wavefronts (plane waves) associated with helicoidal wave modes are observed.

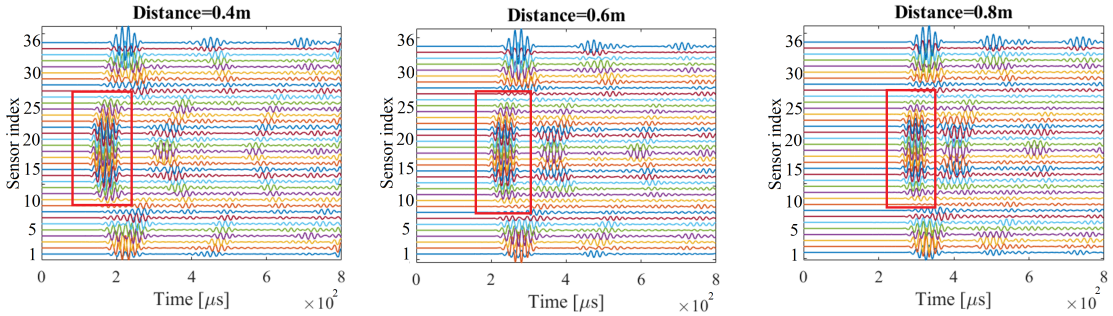

Figure 5. Signals captured by the sensor array for three different axial positions of the discontinuity: (a) 0.4 m, (b) 0.6 m, and (c) 0.8 m.

Two discontinuity locations were considered. First, when the source is located on the same side of the cylinder as the array (zero-order mode). In this case, the array receives the direct wavefront (near field), and beamforming provides the location of the discontinuity. Second, when the source is on the opposite side, outside the direct field of view of the array, the wavefront follows the first-order helical path (far-field). To apply beamforming, a correction that accounts for the angular deviation introduced by helical propagation is performed, since the position of the source is fixed. The signals' apparent arrival angles are corrected by subtracting an angular shift proportional to the number of revolutions, $2\pi R$. Specifically, for each helical order, the corrected angle is calculated as

$$\boldsymbol{\zeta}_r = \boldsymbol{\zeta} - \boldsymbol{k}_r,$$

where $\boldsymbol{\zeta}$ is the helical wavefront direction estimated by beamforming and the $\boldsymbol{\zeta}_r$ vector quantifies the directional mismatch between the estimated wavefront and the true arrival

direction at each sensor and $|\boldsymbol{k}_r| = 2\pi R$. This adjustment aligns all wavefronts with the actual direction of the source, enabling accurate image reconstruction. In Figure 6a, the complete set of signals recorded at the array is shown. Figure 6b shows a closer view of the selected signals, comparing their original form (before correction) and their corrected version. It can be observed how the correction realigns the wavefronts, ensuring that the signals are properly representing the true source direction.

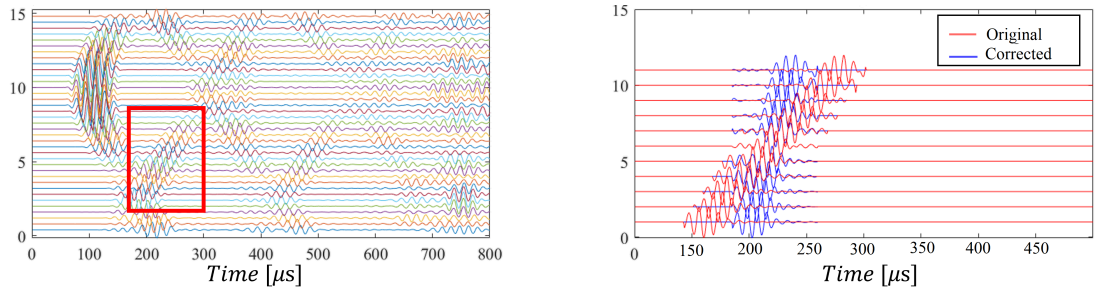

Figure 6. (a) A set of recorded signals by the array, where the window indicating the selected signals for analysis is highlighted. (b) Zoomed view showing the extracted signals before and after the arrival angle correction.

Figure 7 illustrates the beamforming reconstruction results for the two cases discussed. Figures 7a, b are the cylindrical and unwrapped results using direct signals (zero-order); and Figures 7c, d, the corresponding results for the helical mode (first-order mode). For the zero-order wavefront, the localization is determined, while only the direction can be inferred when using helical first-order wavefronts.

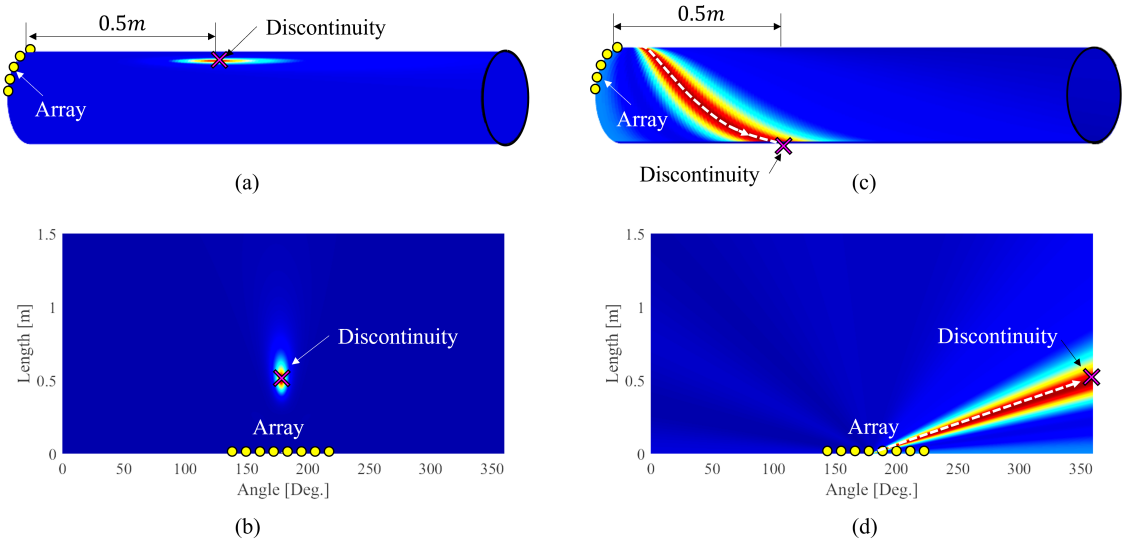

Figure 7. Beamforming reconstruction results using cylindrical and helical wavefronts for a doscontnuity located at 0.5 m for the array (a) 3D view of cilinder and (b) unwrapped 2D map processing the zero-roder wavefront and (c) and (d) processing the first order wavefront.

CONCLUSIONS

In this work, a beamforming-based image reconstruction method for SH0 waves propagating in a cylinder is developed. SH0 waves resulting from the interaction between T(0,1) and a through-hole discontinuity are considered. The scattered wavefield was interpreted as a combination of signals with direct and helical paths. The proposed beamforming allowed imaging of the location and direction of the discontinuity. The method enables source localization using data from only a portion of the cylinder's perimeter, which is relevant for practical applications. Current efforts focus on experimental validation, developing machine learning techniques to automatically identify and separate different wavefronts based on their arrival times and propagation characteristics.

ACKNOWLEDGMENT

The authors would like to thank SECIHTI for the financial support through a doctoral scholarship for Esteban Guerra, which was vital for this research.

REFERENCES

1. Abbas, M. and M. Shafiee. 2018. "Structural health monitoring (SHM) and determination of surface defects in large metallic structures using ultrasonic guided waves," *Sensors*, 18(11):3958.
2. Guan, R., Y. Lu, W. Duan, and X. Wang. 2017. "Guided waves for damage identification in pipeline structures: A review," *Structural control and health monitoring*, 24(11):e2007.
3. Guerra-Bravo, E. and A. Baltazar. 2023. "Excitation of torsional guided waves with flexible PZT transducers in water-filled pipes," *Measurement*, 216:112903.
4. Mitra, M. and S. Gopalakrishnan. 2016. "Guided wave based structural health monitoring: A review," *Smart Materials and Structures*, 25(5):053001.
5. Chua, C. A., P. Cawley, and P. B. Nagy. 2019. "Scattering of the fundamental shear guided wave from a surface-breaking crack in plate-like structures," *IEEE Transactions on Ultrasonics, Ferroelectrics, and Frequency Control*, 66(12):1887–1897.
6. Zhang, X., Z. Tang, F. Lv, and K. Yang. 2017. "Scattering of torsional flexural guided waves from circular holes and crack-like defects in hollow cylinders," *Ndt & E International*, 89:56–66.
7. Fernandez, K., E. Rojas, A. Baltazar, and R. Mijarez. 2021. "Detection of torsional guided wave generation using macro-fiber composite transducers and basis pursuit denoising," *Archive of Applied Mechanics*, 91(5):1945–1958.
8. Wang, H., K. Guo, C. Sun, S. Si, L. Chen, and J. Yang. 2024. "A robust and computationally efficient guided wave tomography of pipes," *Nondestructive Testing and Evaluation*:1–27.
9. Leonard, K. R. and M. K. Hinders. 2005. "Lamb wave tomography of pipe-like structures," *Ultrasonics*, 43(7):574–583.
10. Huthwaite, P. and M. Seher. 2015. "Robust helical path separation for thickness mapping of pipes by guided wave tomography," *IEEE transactions on ultrasonics, ferroelectrics, and frequency control*, 62(5):927–938.
11. Schmidt, R. 1986. "Multiple emitter location and signal parameter estimation," *IEEE transactions on antennas and propagation*, 34(3):276–280.